Carcinogenesis, 2022, **43**, 594–600
https://doi.org/10.1093/carcin/bgac027
Advance access publication 3 March 2022
Original Article

OXFORD

Original Article

The putative oncogenic role of *WDTC1* in colorectal cancer

Xiaoyu Wang[1,2], Qiuyin Cai[1], Jie Ping[1], Hector Diaz-Zabala[1], Yumin Xia[2] and Xingyi Guo[1,3,*]

[1]Division of Epidemiology, Department of Medicine, Vanderbilt Epidemiology Center, Vanderbilt-Ingram Cancer Center, Vanderbilt University School of Medicine, Nashville 37203, TN, USA
[2]Department of Dermatology, The Second Affiliated Hospital of Xi'an Jiaotong University, Xi'an 710004, China
[3]Department of Biomedical Informatics, Vanderbilt University School of Medicine, Nashville, TN, USA

*To whom correspondence should be addressed. Tel: +1-(615)-936-3471; Fax: +1-(615)-343-5938; Email: xingyi.guo@vumc.org
Correspondence may also be addressed to Yumin Xia. Tel/Fax: +86-29-87679969; Email: xiayumin1202@163.com

Abstract

Microsatellite instability (MSI) is detected in approximately 15% of colorectal cancers (CRCs). WD40 and tetratricopeptide repeats 1 (*WDTC1*) is frequently mutated in MSI CRC, indicating that it may contribute to CRC development. However, the functional evidence of the role of *WDTC1* in CRC development remains unknown. Herein, we conducted *in vitro* assays to examine the function of *WDTC1* using knockdown experiments in three CRC cell lines, SW480, CACO2, and LoVo. We provided strong evidence that silencing *WDTC1* significantly suppressed cell proliferation, migration, and invasion consistently in all three CRC cell lines. To evaluate the potential role of *WDTC1* in regulating CRC-related genes, we conducted RNA sequencing after 24 and 48 h in SW480 cells after treating *WDTC1*-siRNA and its vehicle control cells. Differential gene expression analysis identified 44 (42 downregulated and 2 upregulated) and 16 (all downregulated) genes, at time points of 24 and 48 h, respectively, whereas 15 downregulated genes were commonly detected at both time points. The ingenuity pathways analysis suggested that the most significant enrichments associated with cancer function and upstream regulator ATM/ATR were observed for these commonly observed genes. We further verified differential gene expression of eight cancer-related genes, *ARHGEF12, GSTP1, FNDC3A, TMTC3, RTN4, RRM2, UHMK1,* and *PTPRF*, using RT-PCR in all three cell lines. Our findings provided additional insight into the oncogenic role of *WDTC1* in CRC development.

Graphical Abstract

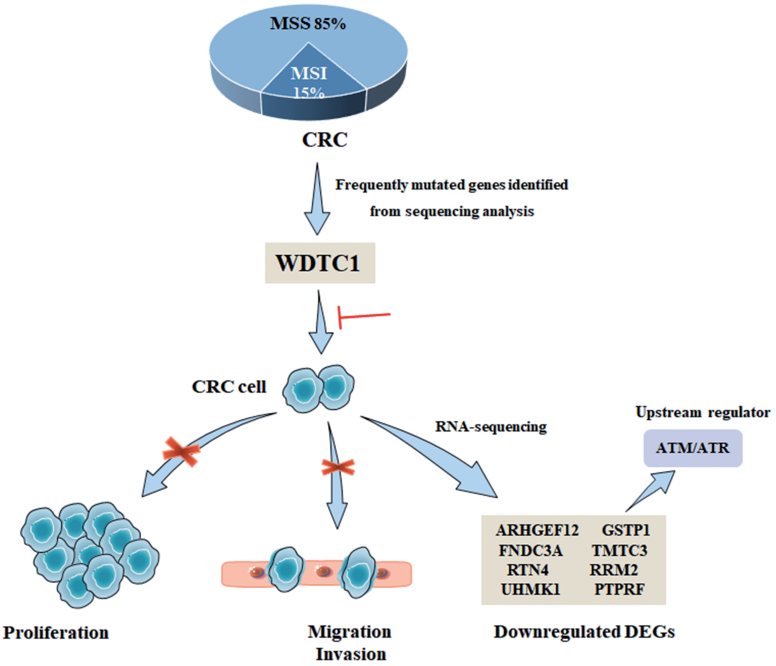

Abbreviations: CRC, colorectal cancer; DEGs, differentially expressed genes; MSI, microsatellite instability; SEM, standard error of mean.

Received: January 13, 2022; Revised: February 16 2022; Accepted: February 28, 2022

Introduction

Colorectal cancer (CRC) ranks fourth in terms of incidence, however, it is the second leading cancer-related cause of death worldwide. More than 1.1 million patients were diagnosed with CRC, and 576 858 deaths occurred in 2020 (1). The incidence of CRC increased while the incidence of other major types of gastrointestinal cancer declined, posing a great challenge to public health (2).

Genetic alterations contribute to the initiation and progression of CRC. As a specific molecular subtype of CRC, microsatellite instability (MSI) presents in approximately 15% of patients with early-stage CRC. It is characterized by DNA mismatch repair system dysfunction, including several established genes (*MLH1, MSH2, MSH6, and PMS2*) (3,4). The MSI in coding regions results in the reformation of the reading frame and the accumulation of errors in protein production (5). Microsatellite instability-high (MSI-H), characterized by harboring higher mutational load, shows unique clinical and pathological features, such as proximal location, poor differentiation, mucinous histology, and a link to BRAF mutations (6). MSI-H CRCs manifest an important immunological response to upregulated immune inhibitory signals, making them prone to immunotherapy with the inhibitors of T-cell checkpoints and display a better prognosis (7).

Mutated genes resulting from the genetic events of MSI are important for the development of CRC both clinically and biologically. Several mutated target genes are well-established driver cancer genes in MSI-H CRC depending on the enriched frequency of mutation, such as *TGFBR2* and *BAX*, which confer oncogenic potential in modulating cellular differentiation, proliferation, and apoptosis (8). In a previous study, numerous novel candidate driver genes with a considerably high somatic mutation frequency were identified utilizing a systematic and unbiased approach, including *GLYR1*, *ABCC5*, *WDTC1*, *ROCK1*, *OR51E2*, and *TCEB3* (9). Among these novel MSI target genes, WD40 and tetratricopeptide repeats 1 (*WDTC1*) was first reported to be associated with MSI CRC. It displayed a typically high mutation frequency of 43% in G8 in 100 MSI CRC samples, indicating a strong potential for the oncogenic involvement in CRC (9).

In previous studies, *WDTC1* emerged as a biomarker of anti-obesity with evidence of lipid accumulation suppression and muFA intake (10-12). Obesity is a major risk factor for CRC development with insulin resistance, aberrant secretion of adipocytokines, and chronic inflammation (13). Despite a conflict between the role of anti-obesity and the potential of the candidate driver genes in MSI CRC, the precise role of *WDTC1* in colorectal carcinogenesis needs to be determined. No study has been reported in the biological function study of *WDTC1* in CRC development. This study was performed to evaluate the role of *WDTC1* in CRC. The effect of *WDTC1* knockdown on cellular proliferation and migration was measured in three CRC cell lines SW480, CACO2, and LoVo. Subsequently, the potential regulatory genes of *WDTC1* in the SW480 cell line was investigated using RNA sequencing analysis and further experimentally verified in SW480, LoVo, and CACO2 cell lines.

Methods

Cell culture

The MSS SW480, CACO2, and MSI LoVo colorectal cancer cell lines were purchased from the American Type Culture Collection (ATCC, VA, USA), and were authenticated using short tandem repeat analysis before performing the experiment. SW480 and LoVo were cultivated in RPMI 1640 (Gibco, CA, USA) supplemented with 10% fetal bovine serum (Gibco). CACO2 was cultured in Eagle's minimum essential medium (EMEM) (Gibco) supplemented with 10% fetal bovine serum. All cell lines were cultured in a humidified incubator at 37°C with 5% CO_2.

Small interfering RNA (siRNA) transfection

The scramble siRNA and three individual siRNAs targeting *WDTC1* (si*WDTC1*-1, si*WDTC1*-2, and si*WDTC1*-3) were purchased from Dharmacon (Dharmacon, CA, USA). RNAiMAX and Lipofectamine 2000 (Invitrogen, CA, USA) were used for siRNA-transfections following the manufacturer's instructions. After performing transfection optimization, SW480, CACO2, and LoVo cells were plated in 96-well plates with a cell density of 6000, 4000, and 4000 per well, respectively. The transfected cells were harvested for further cell viability assays after being cultured in complete medium for 96 h and RT-PCR assay for 36 h.

Cell viability assay

The cell viability was estimated using the Alamar blue assay. On day 1, SW480, CACO2, and LoVo cells were plated in 96-well plates and treated with 10 nM of 3 different target siRNAs. On day 5, Alamar blue was added to the transfected cells with fresh media (1:10 dilution). The plates were incubated at 37°C, and in the presence of 5% CO_2 for 2 h, and then fluorescence (590/530 nm) was detected with a plate reader (BioTek NEO, VT, USA). The experiments were repeated three times.

RNA extraction and real-time PCR

Total RNA from three cell lines was extracted with TRIzol reagent (Invitrogen) following to the manufacturer's protocols and reverse transcribed into cDNA using the High-Capacity cDNA Reverse Transcription Kit (Thermo Fisher Scientific, CA, USA). The cDNA was then amplified using DNA primers and CFX384 Touch Real-Time PCR Detection System (Bio-Rad). The gene expression levels were normalized to GAPDH and the relative expression level was calculated and presented as fold change over control. All primers are listed in Supplementary Table 1, available at *Carcinogenesis* online.

Colony formation assays

The transfected SW480, CACO2, and LoVo cells were seeded in 6-well plates with a density of 1000 cells per well and cultured for 2 weeks. Then, the colonies were fixed with 10% formalin for 30 min and stained with crystal violet (0.1% *w/v*) for at least 15 min. The colonies were scanned and counted using ImageJ analysis.

Migration and invasion assay

Transfected SW480 (4×10^4) and CACO2 (1×10^5) cells were added to the upper chamber with 100 µL of serum-free media, and 600 µL of media containing 20% FBS was filed into the lower chamber. For the migration and invasion assessment, the upper chamber was uncoated or coated with Matrigel (BD Biosciences, CA, USA). After 24 h for migration and 48 h for invasion, the cells in the chamber were fixed with 10% formalin and stained with 0.1% *w/v* crystal violet (Sigma Aldrich, MO, USA) for 30 min. The unbound crystal violet

was removed from inserts and the invaded and migrated cells were quantified and imaged under a microscope. Then, the cells were determined by adding 400 µL of 33% acetic acid into each insert. The fully dissolved crystal violet was collected and transferred to a 96-well plate with gentle shaking for 10 min. The eluent was detected with a microplate reader at 590 nm. Each sample was assayed in triplicate.

RNA-sequencing

Total RNA was extracted from transfected SW480 cells and purified using the TRIzol reagent (Invitrogen) following the manufacturer's instructions. The concentration and quality of the RNA samples were determined using NanoDrop 6000 (Thermo Fisher Scientific). The RNA-seq was conducted by Illumina NovaSeq 6000 with an RNA integrity number greater than 8 for RNA-seq library preparation. The quality control of RNA-seq raw data was performed using FastQC (v1.22.2) (14). RNA-seq sequencing reads were aligned to the human reference genome (hg38) using the STAR two-pass method (15). The gene expression levels were determined from aligned BAM files using featureCounts (16), GENCODE (17) v30 was used for coding genes and noncoding RNA annotations in the human genome. DESeq2 (18) was used to quantify the differential expression genes (DEGs). To identify significant DEGs, we used a threshold of false discovery rate (FDR) <0.05 and log2 fold change (FC) > 1.5. Ingenuity pathways analysis for the significant DEGs was conducted to identify enriched functions and biological relevant pathways.

Statistical analysis

All experiments were conducted in triplicate, and data were presented as the means ± standard error of mean (SEM). Statistical analysis was conducted using GraphPad Prism 5 software (GraphPad Software, CA, USA). Differences between groups or two given groups were analyzed using one-way analysis of variance or *t* tests. Statistical significance was considered upon *P* value <0.05.

Results

Silencing of *WDTC1* inhibited cell proliferation in CRC cell lines

To investigate the function of *WDTC1* in the progression of CRC, the knockdown of *WDTC1* was performed by transfecting three individual siRNAs against *WDTC1* into the SW480, CACO2, and LoVo cell lines. The efficient silence of *WDTC1* at the mRNA level was greater than 80% in three CRC cell lines compared with negative control cells (Figure 1A).

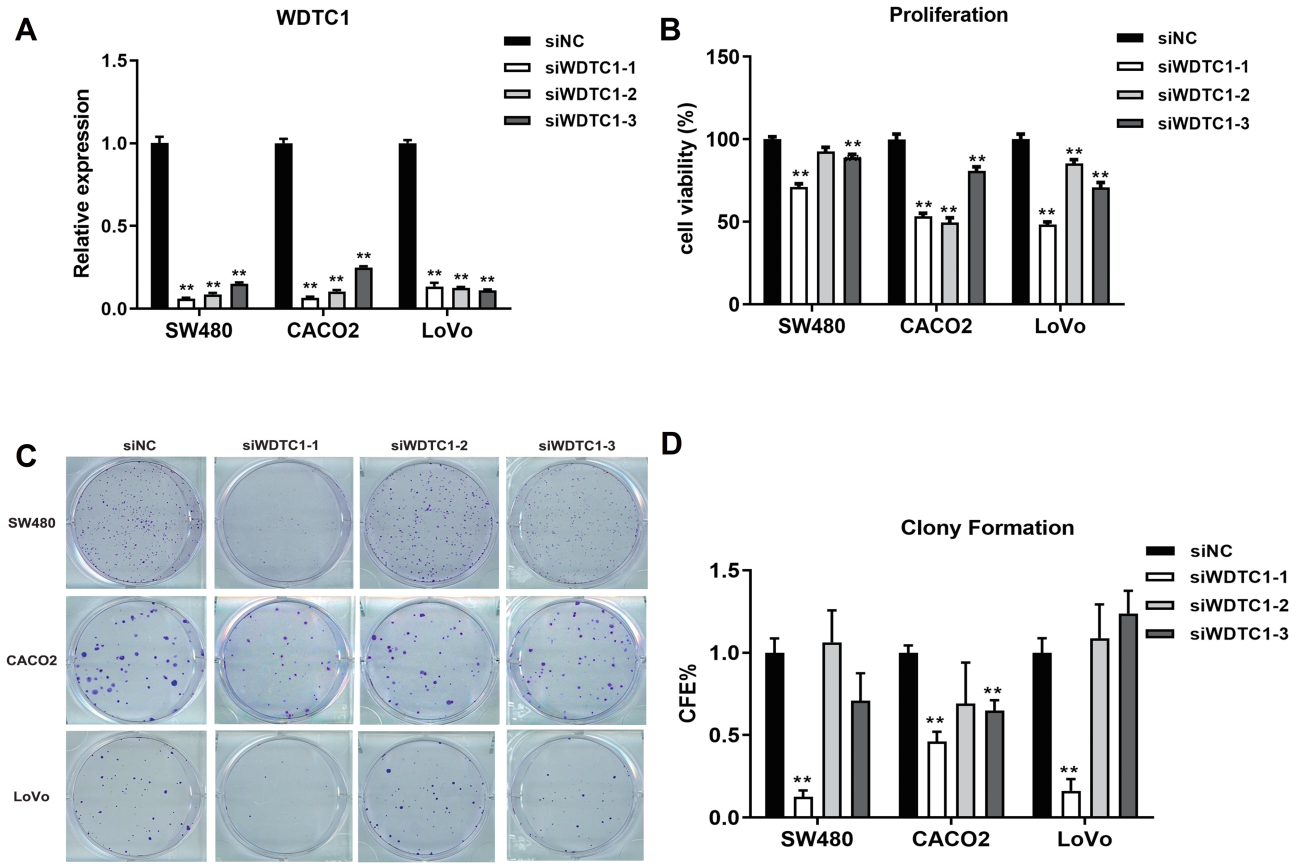

Figure 1. Knockdown of *WDTC1* remarkably inhibited the cell proliferation in CRC cell lines. (A) Transfection with three different individual siRNAs in SW480, CACO2, and LoVo cell lines showed significant efficiency of the silencing of *WDTC1*. (B) Cell viability was measured using Alarmar blue assay in SW480, CACO2, and LoVo cell lines after the knockdown of *WDTC1*. The *WDTC1* siRNA 1 and siRNA 3 consistently inhibited cell viability in three cell lines, while *WDTC1* siRNA 2 showed little effect in SW480 cell line. (C) Colony formation assay conducted in SW480, CACO2, and LoVo cells lines with three different individual siRNAs targeting *WDTC1*. (D) *WDTC1* siRNA 1 remarkably inhibited colony formation in all three cell lines, *WDTC1* siRNA 3 significantly suppressed colony formation in CACO2, while *siWDTC1*-2 showed no effect in three cell lines. Values presented as mean ± SEM. $^{*}P < 0.05$ and $^{**}P < 0.01$ compared with the control.

We next investigated the ability of *WDTC1* in promoting cellular proliferation. We found a 40% reduction in proliferation of *WDTC1*-silenced cell lines compared with the negative control (Figure 1B). The alteration in the proliferative ability of CRC cells was then examined using a colony formation assay. Consistently, the knockdown of *WDTC1* using siRNA 1 decreased the colony formation ability of SW480, CACO2, and LoVo cell lines by 84.8%, 53.8%, and 87.4%, respectively, compared with the negative control (Figure 1C and 1D). Taken together, our results verified the critical effect of *WDTC1* on CRC proliferation *in vitro*.

Knockdown of WDTC1 inhibited cell migration and invasiveness

To further confirm the role of *WDTC1* in cell mobility, we conducted migration and Matrigel invasiveness assays in SW480 and CACO2 cell lines with *WDTC1* siRNA 1 treatment. The silencing of *WDTC1* remarkably decreased the number of penetrated cells by 73.1%, and 65.1%, respectively, in both SW480 and CACO2 cell lines compared with the negative control. As expected, the invasiveness assay revealed that the silencing of *WDTC1* also dramatically inhibited cell invasive capacity in SW480 and CACO2 cell lines by 58.9%, and 42.6%, respectively (Figure 2A and 2B). These results indicated that *WDTC1* promoted the cell migration and invasiveness of CRC *in vitro*.

DEGs were identified upon WDTC1 silencing

To explore the regulatory role of *WDTC1* in CRC, RNA sequencing was performed in both *WDTC1* silencing and control cell lines (see Methods). Subsequently, the differential expression levels of downstream mRNAs in SW480 cells after treatment with *WDTC1* siRNA 1 for 24 and 48 h were compared between the negative control and knockdown groups. All samples showed high quality and consistency with replication (Supplementary Figure 1, available at *Carcinogenesis* online). After 24 h, 44 DEGs were identified by the silencing of *WDTC1* compared with those in scramble control cells, comprising 44 downregulated DEGs and 2 upregulated DEGs. After 48 h, 16 downregulated DEGs were screened out based on the significance criterion (Figure 3A). Among these genes, 15 overlapping DEGs were identified between the two

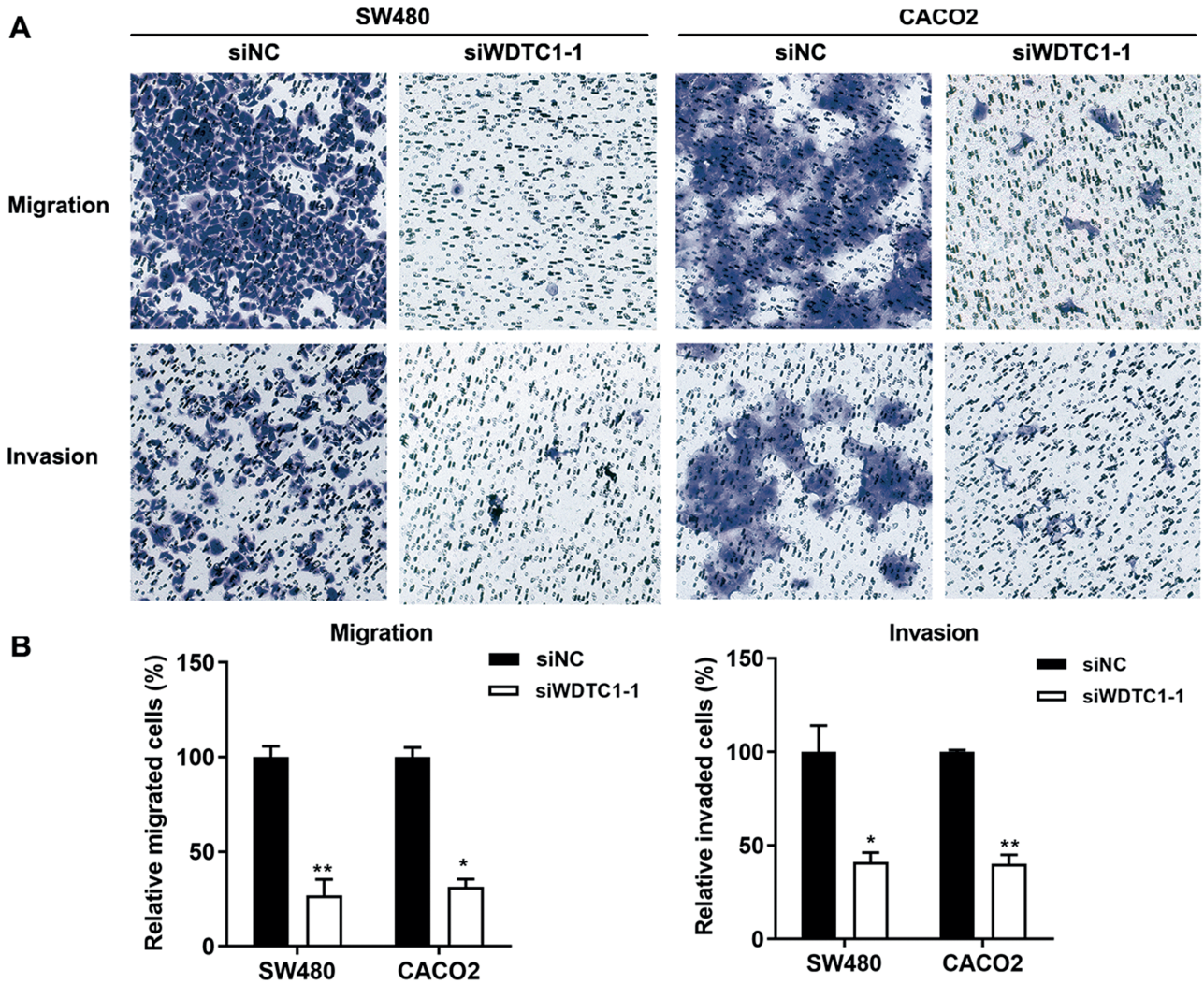

Figure 2. Knockdown of *WDTC1* typically inhibited the cell migration and invasion in CRC cell lines. (A) Cell migration and invasion assay were performed in SW480 and CACO2 cells. (B) Compared with the scrambled siRNA, the *WDTC1* siRNA 1 remarkably suppressed cell migration and invasion in SW480 and CACO2. $^{*}P < 0.05$ and $^{**}P < 0.01$ compared with the control.

time points, and their transcriptional expression was consistently downregulated (Figure 3B). Next, the association between DEGs and related disease and disorders were defined by ingenuity pathways analysis. Our findings revealed that eight genes were highly cancer related, *ARHGEF12*, *GSTP1*, *FNDC3A*, *TMTC3*, *RTN4*, *RRM2*, *UHMK1*, and *PTPRF*, with their upstream regulator being the well-established ATM/ATR (Figure 3B and Supplementary Table 2, available at *Carcinogenesis* online).

The mRNA expression level of eight identified cancer-related DEGs in SW480, CACO2, and LoVo cell lines were detected by RT-PCT after WDTC1 silencing to further validate

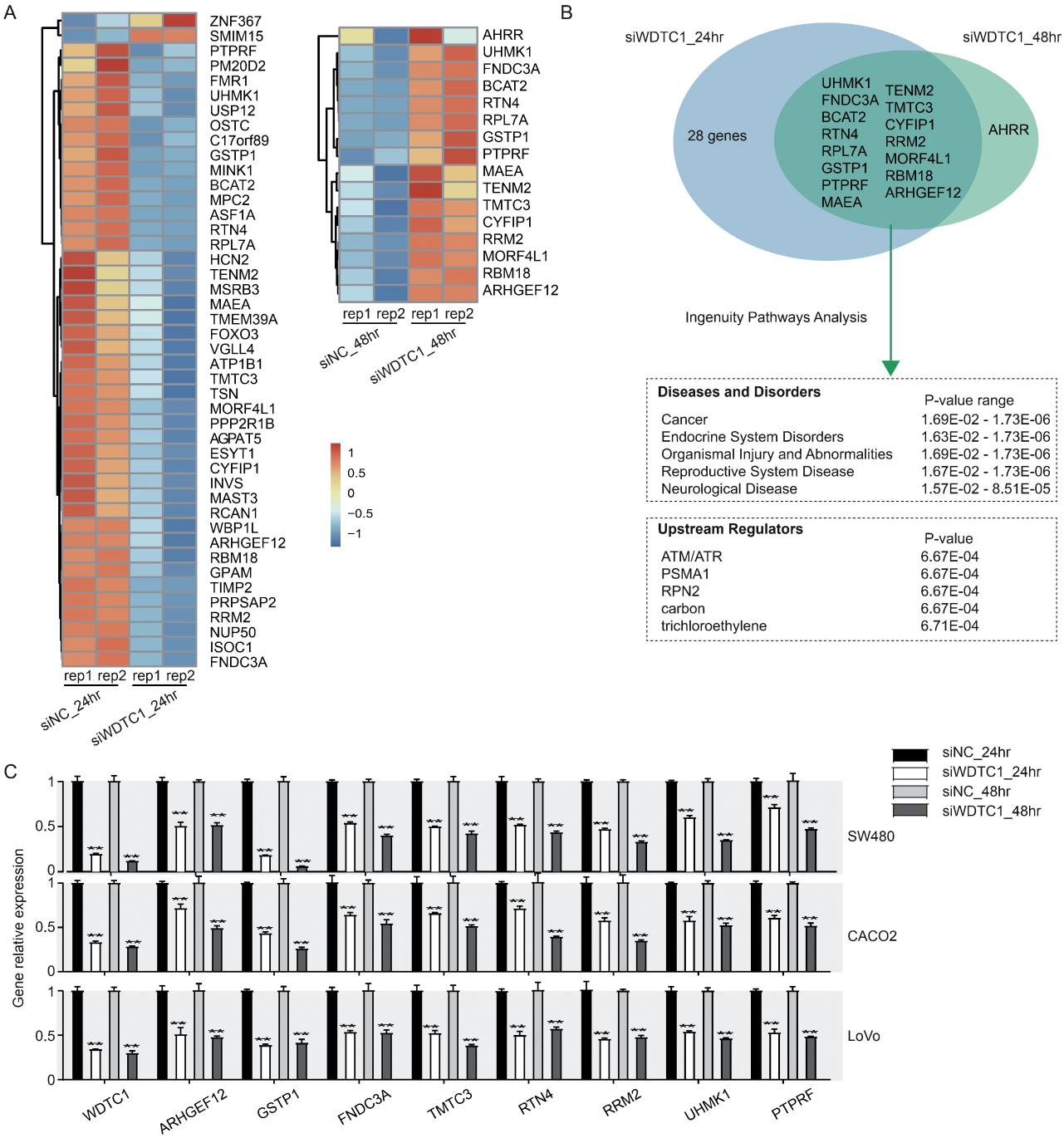

Figure 3. RAN sequencing analysis and RT-PCR validation following the knockdown of *WDTC1* in SW480 cell line for 24 and 48 h. (A) Heat map (left) shows the 44 identified DEGs based on FPKM values by silencing *WDTC1* for 24h, including 44 downregulated DEGs and 2 upregulated DEGs. Heat map (right) represents the 16 downregulated DEGs after silencing *WDTC1* for 48 h. Each column represents the DEGs in different samples with two replicates. Each row represents an individual gene. (B) Venn diagram shows that 15 DEGs were screened out to be overlapping between 24 and 48 h. The annotations of 15 overlapping DEGs to relevant disease and disorders, as well as upstream regulator, were conducted by ingenuity pathways analysis. (C) The mRNA expression of cancer-associated DEGs downregulated by *WDTC1*-silencing was further confirmed by RT-PCR assay in three CRC cell lines. The silencing of *WDTC1* for 24 and 48 h consistently decreased the gene expression of *ARHGEF12*, *GSTP1*, *FNDC3A*, *RTN4*, *RRM2*, *UHMK1*, and *PTPRFF* in SW480, CACO2 and LoVo cells lines. $^{*}P < 0.05$ and $^{**}P < 0.01$ compared with the control.

the expression of identified DEGs in CRC. After 24 and 48 h, the gene expression levels of *ARHGEF12*, *GSTP1*, *FNDC3A*, *TMTC3*, *RTN4*, *RRM2*, *UHMK1*, and *PTPRF* were consistently reduced by more than 50% following the silencing of *WDTC1* in three cell lines (Figure 3C). Collectively, our findings supported the oncogenic potential of *WDTC1* in CRC.

Discussion

MSI, a tumor phenotype with a high level of genomic mutability, has been established as a practicable marker of immunosuppressive therapy and a diagnostic CRC hallmark. Yet the landscape of oncogenes and tumor suppressor mutations remains misunderstood. The excessive genomic instability of MSI CRC led to many putative cancer driver mutations with positive or negative effects on cancer cells in CRC development, such as *SMARCB1, STK38LE, RBB2,* and *HER2,* but many target genes remain functionally unexamined *in vivo* or *in vitro* (19,20). *WDTC1* was first identified as a candidate driver gene in MSI CRC by Alhopuro et al. However, little is known about its biological function in CRC development at present (9). In the present study, we provided the first experimental evidence to support the pro-carcinogenic role of *WDTC1* in two MSS and one MSI CRC cell line. To assess its role in promoting aggressive phenotypes, we performed cell viability and migration assays. The absence of *WDTC1* resulted in a remarkable reduction in CRC cell proliferation, migration, and invasion. Through RNA sequencing analysis and following RT-PCR validation, we presented compelling mechanistic evidence that *WDTC1* played a vital role in modulating the expression of multiple downstream cancer-related genes in CRC cells, including *ARHGEF12*, *GSTP1*, *FNDC3A*, *TMTC3*, *RTN4*, *RRM2*, *UHMK1*, and *PTPRF*. Furthermore, we discovered that the upstream regulator of the overlapping DEGs, ATM/ATR, was a well-known kinase in modulating DNA damage repair and cell cycle. Taken together, our results suggested that *WDTC1* might, as a novel driver gene, play a critical role in the progression of CRC.

We showed that targeting *WDTC1* reduced the expression of eight cancer-related genes, many of which were CRC target genes. For example, *ARHGEF12* and *RTN4* were found to increase cell growth, migration, invasion, and metastasis in CRC cells (21–23). As an isozyme of glutathione S-transferases (GSTs), *GSTP1* was regarded as an enhanced risk factor for CRC, since it promoted carcinogenesis via the F-box only protein 8-GSTP1 axis (24,25). Among the eight genes, fibronectin type III domain-containing 3A (*FNDC3A*) was identified with no previous evidence of involvement in CRC, although its copy number variation enhanced in sporadic CRC (26). Our results provided additional validation for the interaction between *FNDC3A* and CRC advancement that *WDTC1* silencing induced downregulation of *FNDC3A* in CRC cells. *TMTC3* encodes a transmembrane and tetratricopeptide repeat containing three proteins, which was implicated in endoplasmic reticulum stress response in HeLa cells and cell adhesion capacity (27,28). However, the association of *TMTC3* with CRC development was not evaluated in previous studies. Our results provided the first evidence that downregulated *TMTC3* induced by *WDTC1* silencing might decrease cell migration and invasion in CRC cells. The functional analysis of ribonucleotide reductase M2 (RRM2) in CRC showed that *RRM2* was crucial in promoting tumor cell proliferation, migration, and metastasis both *in vitro* and *in vivo* (29,30). As a direct transcriptional target of yes-associated protein (YAP), the positive association between *UHMK1* and *EBLN3P* contributed to the progression of CRC through the mediation of miR-323a-3p (31). We discovered that *PTPRT* was a target in CRC because of its role in preventing cell proliferation, inhibiting tumor initiation, and suppressing the activation of Wnt/β-catenin signaling (32). In addition, we identified the ATM/ATR pathway as the upstream regulator of these commonly detected genes. The increased mutation of ATM/ATR in CRC tumors emerged as therapeutic targets for DNA damage repair inhibitors because of its central role in halting the cell cycle and initiating the response to DNA damage in tumorigenesis (33,34).

Our findings persuasively supported the role of *WDTC1* in facilitating tumorigenesis in both MSI and MSS CRC cell lines. The selection of *WDTC1* as a candidate cancer driver gene reported by Alhopuro et al was based on the frequently somatic mutated in CRC MSI patients, while a low expression of *WDTC1* was observed to be associated with an increased number of mononucleotides repeats based on the data from limited samples (67 MSS and 34 MSI) (9,35). To explore whether *WDTC1* is a potential prognostic biomarker, we additionally evaluated results of survival analysis using gene expression and clinical data of CRC patients from TCGA via UALCAN (http://ualcan.path.uab.edu). Unfortunately, we did not observe statistical evidence of its expression associated with overall survival in CRC patients.

In summary, we provided the biological evidence that *WDTC1* play a vital role in promoting carcinogenesis with consistent results in three CRC cell lines. Our findings further supported the pro-tumorigenic role of *WDTC1* in regulating the expression of multiple downstream cancer-related genes and identified the well-known cancer upstream regulator. This study provided a potential novel interventional target for cancer prevention and precision medicine underlying MSI CRC.

Supplementary material

Supplementary data are available at *Carcinogenesis* online.

Acknowledgements

We thank Rachel Mullen for her assistance in manuscript editing. X.G. was supported by the National Cancer Institute (no. R37CA227130). The RNA-sequencing was supported by The Vanderbilt Institute for Clinical and Translational Research (VICTR) source of Medical Center from Vanderbilt University (no. VR54090).

Author contributions

XG and YX conceived this study. XW performed the experiments and wrote this manuscript. JP and XG conducted the RNA sequencing analysis. QC, HZ, YX and XG discussed, reviewed and revised the manuscript. Study supervision: XG. All authors read and approved the final manuscript.

Data availability

The data generated during the current study are available from the corresponding author on reasonable request.

Conflict of interest

The authors declare no competing interests.

Reference

1. Sung, H. et al. (2021) Global Cancer Statistics 2020: GLOBOCAN estimates of incidence and mortality worldwide for 36 cancers in 185 countries. *CA Cancer J Clin*, 71, 209–249.
2. Arnold, M. et al. (2020) Global burden of 5 major types of gastrointestinal cancer. *Gastroenterology*, 159, 335–349.e15.
3. Dienstmann, R. et al. (2017) Consensus molecular subtypes and the evolution of precision medicine in colorectal cancer. *Nat. Rev. Cancer*, 17, 79–92.
4. Guinney, J. et al. (2015) The consensus molecular subtypes of colorectal cancer. *Nat. Med.*, 21, 1350–1356.
5. Duval, A. et al. (2002) Mutations at coding repeat sequences in mismatch repair-deficient human cancers: toward a new concept of target genes for instability. *Cancer Res.*, 62, 2447–2454.
6. Hu, H. et al. (2013) Clinicopathologic features of synchronous colorectal carcinoma: A distinct subset arising from multiple sessile serrated adenomas and associated with high levels of microsatellite instability and favorable prognosis. *Am. J. Surg. Pathol.*, 37, 1660–1670.
7. Schrock, A.B. et al. (2019) Tumor mutational burden is predictive of response to immune checkpoint inhibitors in MSI-high metastatic colorectal cancer. *Ann. Oncol.*, 30, 1096–1103.
8. Shima, K. et al. (2011) TGFBR2 and BAX mononucleotide tract mutations, microsatellite instability, and prognosis in 1072 colorectal cancers. *PLoS One*, 6, e25062.
9. Alhopuro, P. et al. (2012) Candidate driver genes in microsatellite-unstable colorectal cancer. *Int. J. Cancer*, 130, 1558–1566.
10. Groh, B.S. et al. (2016) The antiobesity factor WDTC1 suppresses adipogenesis via the CRL4WDTC1 E3 ligase. *EMBO Rep.*, 17, 638–647.
11. Galgani, J.E. et al. (2013) Adipose tissue expression of adipose (WDTC1) gene is associated with lower fat mass and enhanced insulin sensitivity in humans. *Obesity (Silver Spring)*, 21, 2244–2248.
12. Lai, C.Q. et al. (2009) WDTC1, the ortholog of *Drosophila* adipose gene, associates with human obesity, modulated by MUFA intake. *Obesity (Silver Spring)*, 17, 593–600.
13. Bardou, M. et al. (2013) Obesity and colorectal cancer. *Gut*, 62, 933–947.
14. Andrews, S. (2010) *FastQC: A Quality Control Tool for High Throughput Sequence Data*. http://www.bioinformatics.babraham.ac.uk/projects/fastqc/.
15. Dobin, A. et al. (2013) STAR: ultrafast universal RNA-seq aligner. *Bioinformatics*, 29, 15–21.
16. Liao, Y. et al. (2014) featureCounts: an efficient general purpose program for assigning sequence reads to genomic features. *Bioinformatics*, 30, 923–930.
17. Frankish, A. et al. (2019) GENCODE reference annotation for the human and mouse genomes. *Nucleic Acids Res.*, 47, D766–D773.
18. Love, M.I. et al. (2014) Moderated estimation of fold change and dispersion for RNA-seq data with DESeq2. *Genome Biol.*, 15, 550.
19. Kloth, M. et al. (2016) Activating ERBB2/HER2 mutations indicate susceptibility to pan-HER inhibitors in Lynch and Lynch-like colorectal cancer. *Gut*, 65, 1296–1305.
20. Kondelin, J. et al. (2018) Comprehensive evaluation of coding region point mutations in microsatellite-unstable colorectal cancer. *EMBO Mol. Med.*, 10, e8552.
21. Shi, G.X. et al. (2018) RSK2 drives cell motility by serine phosphorylation of LARG and activation of Rho GTPases. *Proc. Natl. Acad. Sci. U.S.A.*, 115, E190–E199.
22. Xue, H. et al. (2015) Knockdown of reticulon 4C by lentivirus inhibits human colorectal cancer cell growth. *Mol. Med. Rep.*, 12, 2063–2067.
23. Bateman, L.A. et al. (2017) Chemoproteomics-enabled covalent ligand screen reveals a cysteine hotspot in reticulon 4 that impairs ER morphology and cancer pathogenicity. *Chem Commun (Camb)*, 53, 7234–7237.
24. FeiFei, W. et al. (2019) FBX8 degrades GSTP1 through ubiquitination to suppress colorectal cancer progression. *Cell Death Dis.*, 10, 351.
25. Ding, F. et al. (2018) Comprehensive analysis of the association between the rs1138272 polymorphism of the GSTP1 gene and cancer susceptibility. *Front. Physiol.*, 9, 1897.
26. Shivakumar, B.M. et al. (2016) Comparative analysis of copy number variations in ulcerative colitis associated and sporadic colorectal neoplasia. *BMC Cancer*, 16, 271.
27. Racape, M. et al. (2011) The involvement of SMILE/TMTC3 in endoplasmic reticulum stress response. *PLoS One*, 6, e19321.
28. Graham, J.B. et al. (2020) Endoplasmic reticulum transmembrane protein TMTC3 contributes to O-mannosylation of E-cadherin, cellular adherence, and embryonic gastrulation. *Mol. Biol. Cell*, 31, 167–183.
29. Chen, C.W. et al. (2019) DHS (trans-4,4'-dihydroxystilbene) suppresses DNA replication and tumor growth by inhibiting RRM2 (ribonucleotide reductase regulatory subunit M2). *Oncogene*, 38, 2364–2379.
30. Liu, Q. et al. (2021) A MYBL2 complex for RRM2 transactivation and the synthetic effect of MYBL2 knockdown with WEE1 inhibition against colorectal cancer. *Cell Death Dis.*, 12, 683.
31. Xu, X.H. et al. (2021) Long non-coding RNA EBLN3P regulates UHMK1 expression by sponging miR-323a-3p and promotes colorectal cancer progression. *Front Med (Lausanne)*, 8, 651600.
32. Gan, T. et al. (2020) Inhibition of protein tyrosine phosphatase receptor type F suppresses Wnt signaling in colorectal cancer. *Oncogene*, 39, 6789–6801.
33. Pilie, P.G. et al. (2019) State-of-the-art strategies for targeting the DNA damage response in cancer. *Nat. Rev. Clin. Oncol.*, 16, 81–104.
34. Parikh, A.R. et al. (2019) Analysis of DNA damage response gene alterations and tumor mutational burden across 17,486 tubular gastrointestinal carcinomas: implications for therapy. *Oncologist*, 24, 1340–1347.
35. Kruhoffer, M. et al. (2005) Gene expression signatures for colorectal cancer microsatellite status and HNPCC. *Br. J. Cancer*, 92, 2240–2248.